ELSEVIER

Nuclear Instruments and Methods in Physics Research A 431 (1999) 123–133

NUCLEAR INSTRUMENTS & METHODS IN PHYSICS RESEARCH Section A

www.elsevier.nl/locate/nima

A large-acceptance spectrometer for tracking in a high-multiplicity environment, based on space point measurements and high-resolution time-of-flight

L. Carlén[a], K. El Chenawi[a], T. Chujo[b], K. Enosawa[b], S. Garpman[a], H.-Å. Gustafsson[a], M. Kurata[b], K. Kurita[b], H. Löhner[c], M. Martin[d], Y. Miake[b], Y. Miyamoto[b], H. Naef[d], P. Nilsson[a], S. Nishimura[b], J. Nystrand[a], A. Oskarsson[a], L. Österman[a], I. Otterlund[a], E. Perrin[d], L. Rosselet[d], J.M. Rubio[d], H. Sako[b], S. Sato[b], D. Silvermyr[a,*], K. Söderström[a], N. Solomey[d], E. Stenlund[a], T. Svensson[a], S. Vörös[d], K. Yagi[b], Y. Yokota[b]

[a]*Department of Physics, Division of Cosmic and Subatomic Physics, Lund University, Box 118, SE-22100 Lund, Sweden*
[b]*University of Tsukuba, Tennoudai, Tsukuba 305, Japan*
[c]*KVI, University of Groningen, NL-9747 AA Groningen, The Netherlands*
[d]*University of Geneva, CH-1211 Geneva 4, Switzerland*

Received 12 February 1999; accepted 26 February 1999

Abstract

A large acceptance tracking system, specially developed for tracking at very high particle densities encountered in ultra-relativistic heavy-ion collisions is described. The system is a combination of multi-step avalanche chambers equipped with electronic pad readout with high position resolution in two dimensions and streamer-tube detectors with pad readout, with coarser position resolution, that is sufficient for safe pattern recognition. A high-resolution time-of-flight system (time resolution better than 90 ps) provides particle identification up to 8 GeV/c for pions and protons and pion/kaon separation up to 4 GeV/c. All detectors in the tracking system are read out with new, high-performance integrated circuits. The system can operate at high event rates due to efficient zero suppression. The performance of the system for tracking under real running conditions with Pb-beam at 158 A GeV in the WA98 experiment at CERN is presented.

PACS: 29.40.CS; 29.40.GX; 29.40.MC; 29.30.AJ

Keywords: Multi-step avalanche chamber; Pad readout; Streamer tubes; Time-of-flight; Tracking; Particle identification

1. Introduction

The use of heavy nuclei as projectiles in experiments at ultra-relativistic energies at the SPS presents new experimental challenges due to the very

* Corresponding author. Tel.: + 46-46-222-7704; fax: + 46-46-222-4015.
E-mail address: david@kosufy.lu.se (D. Silvermyr)

0168-9002/99/$ - see front matter
PII: S0168-9002(99)00261-2

large particle multiplicities, which are an order of magnitude larger than encountered with light-ion beams.

Some types of measurements, e.g. with high-resolution electromagnetic calorimeters, can only cope with the high particle density by increasing the distance to the target since the shower diameter is fixed for a given material. Charged particle tracking, on the other hand, has to be performed as close as possible to the target, in order not to destroy the resolution by multiple scattering. In typical tracking detectors, e.g. gaseous ionization detectors, the ionization event in the gas has very small dimensions. Thus a very high track density can be handled by increasing the granularity in the readout system.

In order to resolve tracks at high multiplicity it is necessary to trace the particles in all three dimensions. In a Time Projection Chamber (TPC), the tracking in three dimensions is exploited to the limit with a continuously recorded track image. A drawback of the TPC is long drift times limiting its use at high collision rates. Thus other methods have to be developed, suitable for use in studies of rare signals. Planar tracking stations using crossed planes of tracking detectors which are position sensitive in only one dimension are inadequate due to combinatorial ambiguities in the determination of the coordinates along a track.

The system described here uses planar tracking detectors with short drift time and position readout in two dimensions. The target–detector distance provides the third coordinate. This technique allows data taking at high collision rates and preserves the good track recognition characterizing tracking in three dimensions.

The system is based upon Multi-Step Avalanche Chambers (MSACs) equipped with an ultra-thin electronic pad readout system with a very large number of channels. These detectors, in the text referred to as "pad chambers", give precise coordinates for momentum measurements while two planes of streamer tube detectors with pad readout provide a coarser coordinate measurement, adequate for track recognition. These systems use a new, specially developed integrated circuit which is used for readout of 83 000 channels in this detector system. The particle identification is done with a high-resolution Time-Of-Flight (TOF) detector based on plastic scintillators, read out by Photo-Multiplier-Tubes (PMTs). The readout electronics is based on two custom-made chips, the Time-to-Voltage Converter (TVC) and the Charge-to-Voltage Converter (QVC), both equipped with a switched capacitor Analog Memory Unit (AMU).

The tracking system was implemented as the second tracking arm (Fig. 1) in the WA98 experiment and it was used for the first time with the Pb-beam at 158 A GeV at the SPS in 1996. The first tracking arm in WA98 used the same tracking philosophy with planar, large-area detectors read out in two dimensions with a very large number of pixels. These detectors are MSACs read out with CCD cameras, equipped with image intensifiers.

The aperture of the second arm tracking system is large, typically allowing about 30 particles per central event to be traced. Thus it is possible to obtain good statistics for single particle observables, and excellent performance can be achieved in studies involving particle correlations, e.g. like-particle intensity interferometry and resonance decay. Recent analysis of the data has shown that it is feasible to reconstruct the Δ^{++} resonance decaying into a pion and a proton [1]. In combination, the two arms allow measurements of decaying resonances into a positive and a negative particle. A particular focus of the experiment is to study the properties of the ϕ-meson from its decay into K^+K^-.

The three detector systems in the second tracking arm are new developments which utilize advanced and unique readout solutions with specially designed integrated circuits which are used here for the first time. The details of the detector systems have been extensively described in separate publications [2–4], while this paper concentrates on the performance of the system as a whole.

2. The detectors in the second tracking arm

The detector components in the second tracking arm are two planes of pad chambers, two planes of streamer-tube detectors with pad readout and one plane of time of flight detectors. Fig. 2 shows

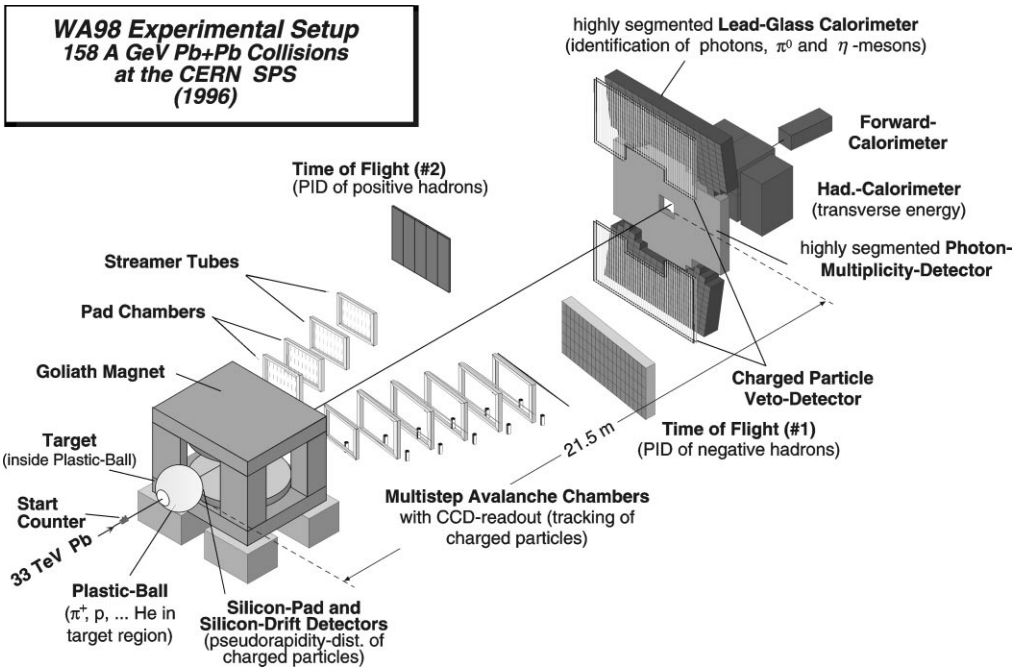

Fig. 1. WA98 experimental setup.

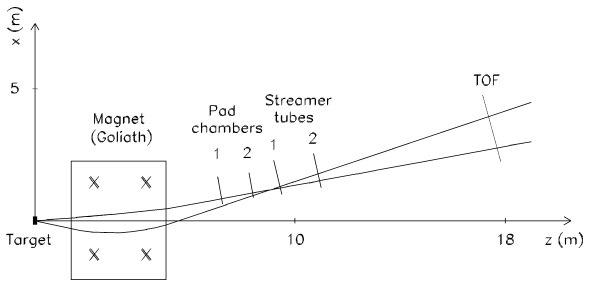

Fig. 2. Overview of the second tracking arm detector system. The flight path from the target to the TOF wall is about 18 m.

a schematic top view of the tracking system. The location of the tracking stations with respect to the target and the magnet are indicated. The passage of a high-momentum particle with positive p_x and a low-momentum particle with a negative p_x through the system is also shown. Outside the magnetic field, the particles move in straight lines.

All five planes provide space coordinates for the traversing particles. The two planes of pad chambers (separated by 1.2 m) determine the direction of each track with high resolution for precise momentum measurements while the two planes of streamer-tube detectors and the TOF wall have sufficient position resolution for safe track reconstruction and for acceptable momentum resolution even if one of the pad chambers is desensitized due to a spark.

2.1. The multi-step avalanche chambers with electronic pad readout

The novel readout concept used in conjunction with the pad chambers is based on a custom-designed chip containing both analog and digital functions as well as ultra-thin mounting with the chip-on-board technique [3]. The detection efficiency of the chambers, when they are not affected by a spark, is in the range of 91–96% [4].

The intrinsic position resolution is 0.5 mm in the horizontal direction and 1.7 mm in the vertical direction [4]. Due to the long flight path (7 m) from the target to the first pad chamber plane we find

that the position resolution is limited by multiple scattering rather than the intrinsic position resolution of the detectors. The good position resolution is of great value in the tracking, since the multiple scattering between the pad chamber planes is small, thus allowing restrictive cuts in the track fitting, which is essential for tracking at high multiplicity.

2.2. The streamer-tube detectors with pad readout

Streamer-tube detectors are in widespread use in high-energy physics experiments due to their low cost, high gain and rugged construction suitable for large area coverage. Such detectors equipped with pad readout have been used in the earlier generations of the WA98 experiment (WA80 [5] and WA93 [6]), as large-area charged-particle multiplicity detectors with moderate position resolution. The streamer tubes were then operated at very high gain which allowed readout without further amplification. The amplifier stage of the readout chip developed for the pad chambers was modified in order to make it suitable for readout of pads on the streamer-tube detectors [2]. The streamer tubes could then be operated at lower gain, resulting in more stable operating conditions, still maintaining high efficiency of 90–98%.

A printed circuit board, with the sensor pads on one side and the readout chips with supply and readout lines on the other, is attached to the streamer-tube module. The streamer tubes were 1.20 m long and each module contained 8 wire tubes (Fig. 3).Three connected circuit boards cover the full length of a streamer tube. The readout chips of several streamer-tube modules were connected together to form a long readout chain delivering data to the Digital Signal Processor (DSP) boards. These are of the same design and fabrication as used for the pad chambers [3].

A large array of these streamer-tube detectors was also used as a charged particle veto detector in front of the high-resolution lead glass calorimeter (Fig. 1). The streamer-tube detectors in the second tracking arm were read out with rectangular pads ($7 \times 22\,\mathrm{mm}^2$) with the longest side parallel to the tube. The detector modules were positioned at 30° with respect to the detector plane. This served the purpose of minimizing the risk that a particle passes through the tube walls only and not through the gas. These walls occupy 10% of the streamer

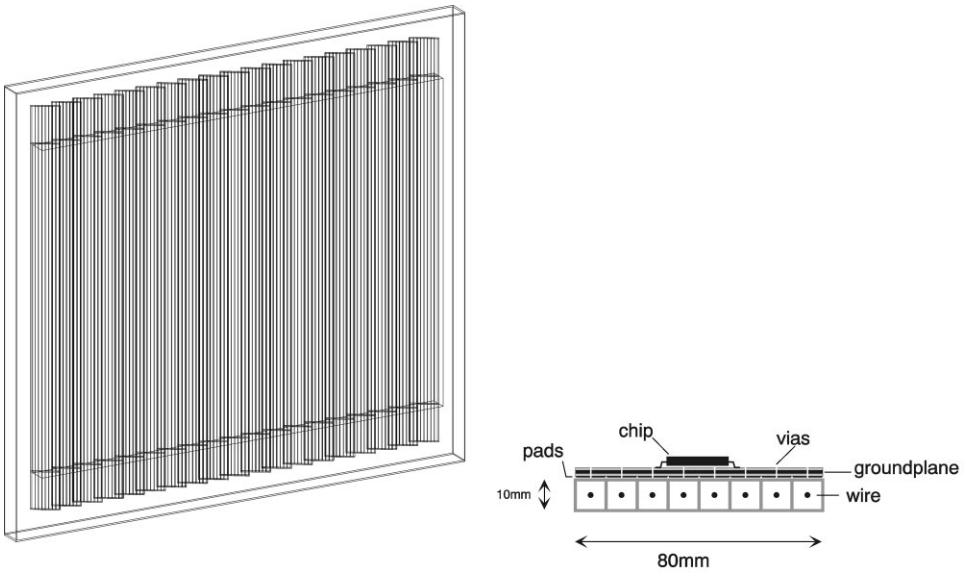

Fig. 3. The streamer-tube detector plane consisting of 19 streamer tubes, tilted with respect to the detector plane, and a cut view of one streamer tube.

tube width. The resolution across the wires is in the first approximation determined by the wire distance (the tube pitch is 10 mm), but improved by the tilted arrangement of the detector modules. With the pulse height measurement, it was possible to determine the avalanche positions along the wires with fairly good resolution. The position resolution achieved in the streamer-tube planes has been found to be 3 mm in the horizontal and 6.5 mm in the vertical direction.

2.3. The time-of-flight detectors

The time-of-flight of detected particles provides particle identification when combined with the momentum information. The flight path is about 18 m and together with the extremely good time resolution (better than 90 ps) this allows particle separation at the 4σ level, up to 4 GeV/c for π/K separation and up to 8 GeV/c for π/p identification.

The time-of-flight measurement is started by a gas Cherenkov counter placed in the beam (time resolution 30 ps [7]) about 1 m upstream from the target. The beam intensity with Pb ions is a few 10^5 ions/s which allows time measurement for the passage of individual beam particles. From this setup the time of the collision in the target is obtained.

The TOF wall (Fig. 4) covers an area 2450 mm wide (160 columns of scintillators) and 1924 mm high (3 rows of scintillators). Therefore, the area is filled with 480 slats of scintillators (BICRON, BC404, 1.5 cm in width, 1.5 cm in depth). Each scintillator slat has PMTs (Hamamatsu, R3478s) on both ends. Scintillators with two different lengths (637.7 and 433.9 mm) are assembled in an alternating fashion in order to avoid geometrical conflicts between the PMTs of neighboring slats.

The TOF wall and its electronics is primarily designed to be used in the PHENIX experiment at RHIC [8]. The front-end electronics of the TOF wall was designed to sample the TOF signals at the bunch crossing frequency (9.4 MHz) of RHIC and to store them during the first-level trigger latency of 4.24 μs, corresponding to 40 RHIC bunch crossings. The signal timing from the PMT is determined by a leading edge discriminator followed by a TVC. The charge information is converted to a voltage by a QVC. The analog voltages from the TVC and the QVC are stored by a switched capacitor AMU which stores the information during the latency and buffers up to five accepted events. The stored voltages are digitized by a 12 bit 1.25 MHz ADC.

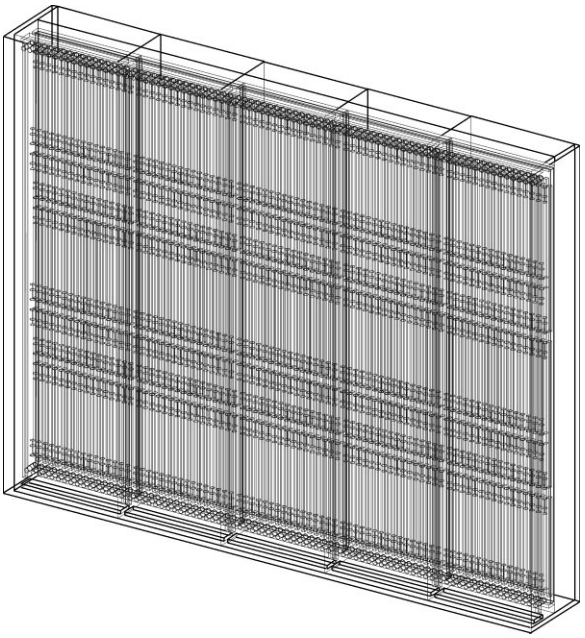

Fig. 4. The time-of-flight detector as it is modeled in GEANT. It consists of five panels, each with 32 columns and 3 rows of scintillators, resulting in a total of 480 scintillator slats.

The hit position in the vertical direction (along the slats) is derived from the time and amplitude difference observed in the signals, read out in the two ends of the slat. The tracking analysis has revealed a position resolution in the TOF wall of 12.5 mm in the horizontal and 26.4 mm in the vertical directions.

3. Track reconstruction

The track reconstruction procedure has two steps. In the first step, each detector plane is analyzed separately, clusters of fired pads are identified and the information is translated to a global x–y coordinate for each potential hit. Each hit in the four tracking planes (pad chamber 1,2 and streamer

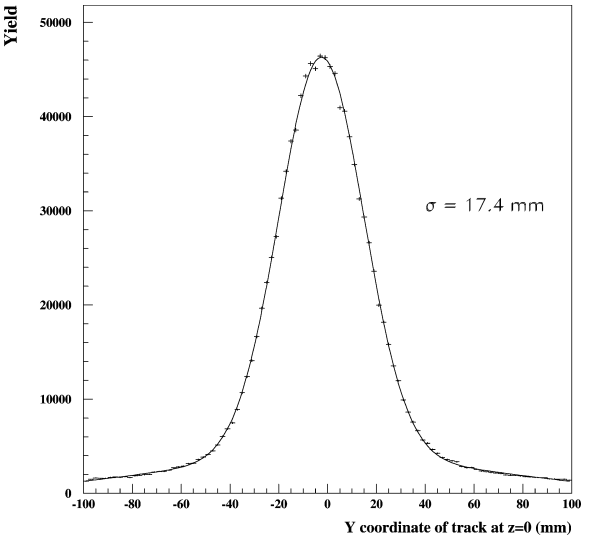

Fig. 5. Reconstructed target vertex (vertical projection), obtained by trace back of all found tracks to the z-coordinate of the target.

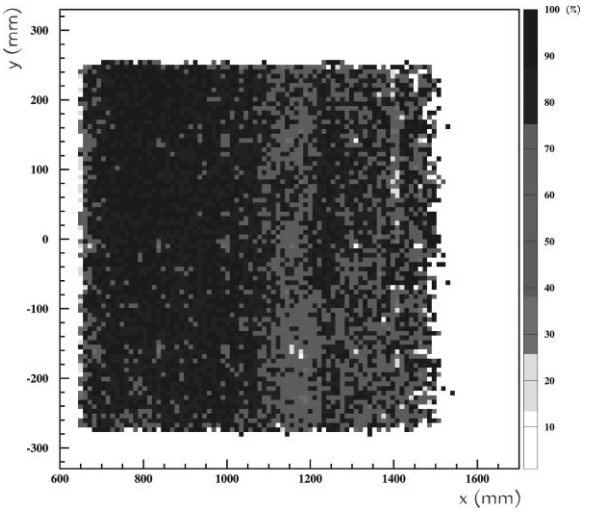

Fig. 6. The local efficiency of pad chamber 1. Black represents the highest efficiency. The reduced efficiency due to a spacer is e.g. seen at (840,140). The spacers form a regular pattern with a 15 cm spacing

tube 1,2; see Fig. 2) is characterized by the number of fired pads and the total charge in the cluster. In the second step, the tracks are found by straight-line fitting to the obtained hit coordinates in at least three of the four tracking planes.

Fig. 5 shows the distribution at the vertical coordinate at the target for reconstructed tracks. The width of the distribution has contributions from the finite size of the target spot (roughly 5 mm), the vertical position resolution of the tracking chambers, multiple scattering and non-vertical components of the magnetic field. The restrictive traceback to the target spot effectively eliminates background from secondary particles produced at the magnet poles, and also ensures reliable track recognition when only three tracking chambers register the track.

Some reconstructed clusters may be due to neutral particles (neutrons, γ- or X-rays). Although the detection probabilities for neutral particles are small in gaseous chambers, this background (which does not form tracks) is sizeable due to the large production cross section in heavy-ion collisions. Due to the good space resolution, allowing very restrictive definition of tracks, this background has not been any significant problem in the tracking.

The high quality of the track finding is illustrated in Fig. 6 which shows the local efficiency over the area in pad chamber 1. The efficiency is determined by projecting all tracks with particle identification found by coordinates in pad chamber 2, streamer-tube detectors 1 and 2, into pad chamber 1. The probability that a hit is found in pad chamber 1, within a radius of 10 mm (based on the expected position resolution) around the predicted hit coordinate is calculated. The result is corrected for random hits.

The average efficiency over the whole chamber is about 85%. The apparent, general efficiency variation in x, is a consequence of the fluctuations owing to decreasing statistics at large x (large angles). A real reduction in efficiency is observed around $x = 1150$. This is due to unstable running conditions in the readout electronics.

The small white/grey spots (inactive areas) forming a regular pattern illustrate the tracking accuracy. These spots correspond to the positions in pad chamber 1 where the passage of the electron clouds are blocked by spacers between the meshes. The spacers are used to keep the meshes flat and parallel to each other to have a uniform response

over the whole detector area. The chamber is thus insensitive at these spots.

To estimate the accidental background contribution to the track distribution, two different approaches were pursued. In the first one, an event-mixing technique was utilized. We used the hit information from the four tracking planes and the TOF wall from five different central events of approximately the same multiplicity to reconstruct the tracks. The same reduced χ^2 (<2.5) and target-association cuts (± 50 mm, see Fig. 5) were applied to the data as well as to the mixed events. It was observed that the contribution from the event-mix relative to data was less than 7% for three-chamber tracks and about 0.1% for four-chamber tracks. If we also require particle identification, the background contribution for three-chamber tracks is reduced to about 2%.

In the second approach, central Pb–Pb events from the RQMD [9] event generator were filtered through the acceptance of the GEANT [10] simulation package. The coordinates from charged pions, kaons and protons traversing at least three out of the four tracking planes and the TOF wall were saved and given as input to the WA98 analysis package. According to the measured average position resolution the hit positions were modified by a Gaussian smearing function, and fake clusters were added. Taking into account the measured chamber efficiencies, a number of good hits were deleted randomly before reconstructing tracks. The obtained number of reconstructed tracks per event is compared with data in Fig. 7. The same cuts as above for the χ^2 and target association have been applied. The track multiplicity from simulations differs from the data by about two tracks per event. The ratio between incorrectly and correctly reconstructed track from RQMD is about 7% for three-chamber tracks after these cuts, in agreement with what was found using the mixed event technique described above.

The data used to determine the tracking quality has been acquired with a trigger on central Pb–Pb collisions, i.e. with many tracks passing through the tracking system. Data was acquired at a rate of about 50 central events per second in spite of the very large number of detection channels (83 000). This was possible due to the powerful suppression

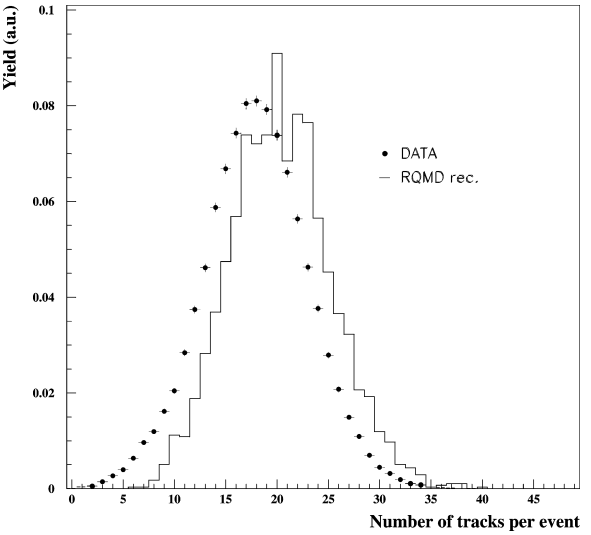

Fig. 7. The multiplicity of reconstructed tracks per event. Data are compared with RQMD events which were filtered through the GEANT acceptance and reconstructed in the same manner as data.

of data from empty channels in parallel processing at an early stage of the data readout chain. The data rate corresponds to about 1000 recorded tracks per second. The major rate limitation in this experiment was the spark rate (about 1 spark per 100 events) in the pad chambers which had to be kept at a level where the balance between dead time after a spark and the amount of data collected was optimal.

4. Momentum determination and resolution

Using the direction vector of the found track, the momentum of the detected particle can be determined by tracing the track through the known magnetic field of the Goliath dipole-magnet (1.6 Tm). The GEANT simulation package was utilized to estimate the momentum resolution. Particles with known momenta were randomly generated at the target position. If the tracks passed through at least three out of the four tracking planes, the coordinates of the hits were stored. These coordinates, modified by a Gaussian smearing function according to the measured average

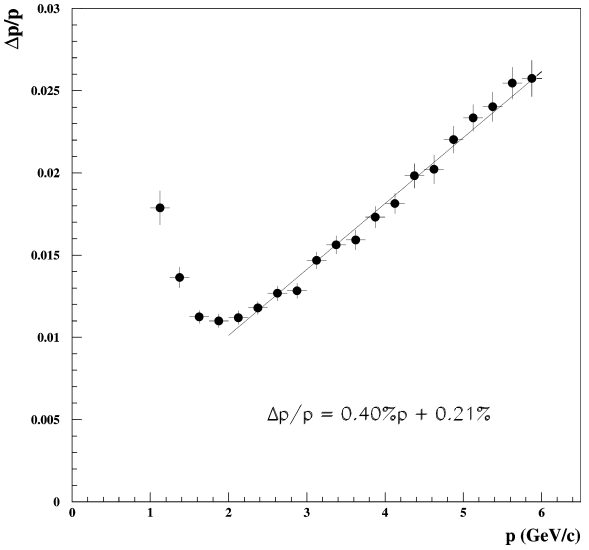

Fig. 8. The relative momentum resolution $\Delta p/p$ as a function of the particle momentum p.

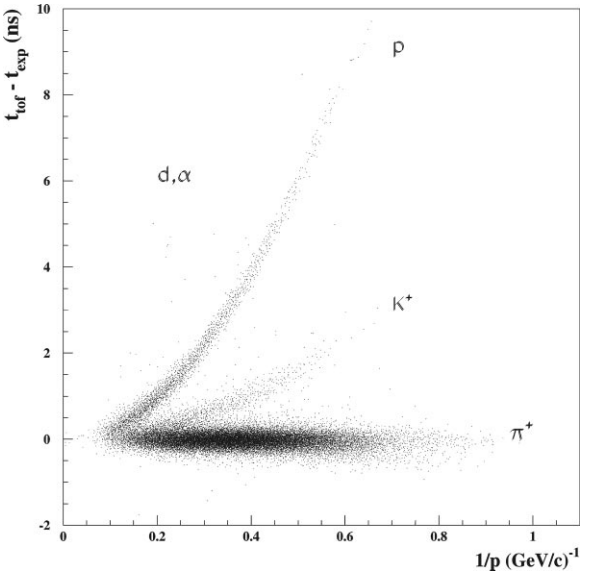

Fig. 9. The difference between the measured (t_{tof}) and expected time (t_{exp}), assuming pion mass as a function of the inverse momentum.

position resolution of the different detectors, were then given as input to the WA98 analysis package including the measured magnetic-field map. The calculated relative momentum resolution $\Delta p/p$, in the momentum range $1 \leq p \leq 6$ GeV/c is shown in Fig. 8.

5. Particle identification

The number of particles with multiple charge entering the tracking system is negligible. Thus particle identification can be restricted to mass separation among singly charged (negative or positive depending on the magnetic field orientation) particles. This is achieved by combining the information of the momentum and velocity measurements. The expected flight time was calculated from the track length (r_{track}), momentum and mass of the particle in the following way:

$$t_{\mathrm{exp}} = \frac{r_{\mathrm{track}}}{c}\sqrt{1+\left(\frac{m_0 c}{p}\right)^2}. \qquad (1)$$

The expected time of flight t_{exp} has been calculated on the basis of the reconstructed particle momentum assuming that all particles are pions. Among the positively charged particles one can recognize in Fig. 9 the bands of pions, kaons, protons and possibly deuterons inside the acceptance. The lightest particles, the pions, travel with almost the speed of light for all momenta inside the acceptance.

For particle separation, cuts have been applied on the time-difference variable ($t_{\mathrm{tof}} - t_{\mathrm{exp}}$) which is calculated from the measured and expected time of flight. The flight-time differences for assumed pion (a), kaon (b) and proton (c) masses are shown in Fig. 10 as a function of the particle momentum. The correct particles are found in narrow bands at small time differences. Pions and kaons are no longer separable at momenta above 4 GeV/c. For correctly assumed particle identity the expected time equals the measured time independently of the momentum. From this observation we conclude that the time and momentum calibrations are consistent.

6. Two-track resolution

The fine granularity of the pad chambers allows good performance for tracks passing close to each

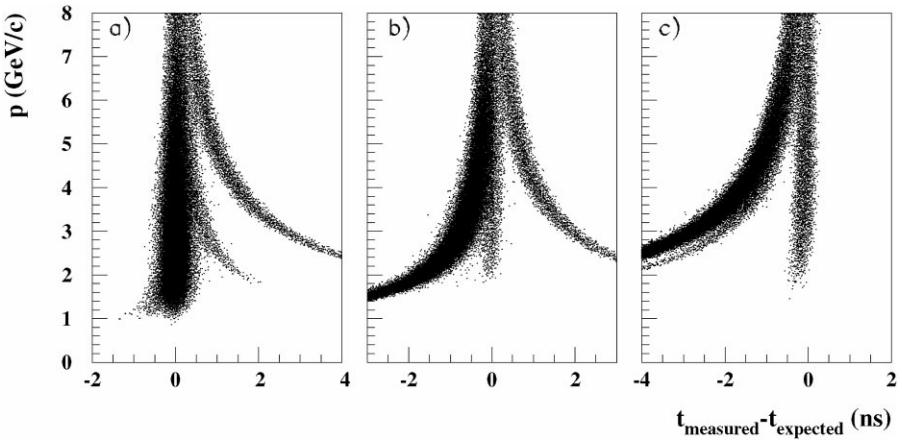

Fig. 10. Particle identification, exploiting the time-of-flight differences shown in Fig. 9 and assuming (a) the pion mass, (b) the kaon mass and (c) the proton mass.

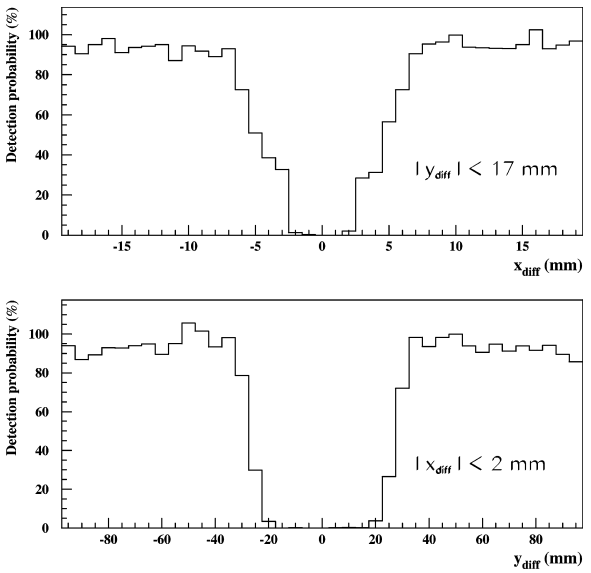

Fig. 11. The detection probability as a function of distance between the chamber coordinates in horizontal (upper panel) and vertical (lower panel) direction of an observed track and all other nearby tracks. The vicinity of tracks is defined by the indicated window in the respective other coordinate.

other in a chamber. This property is of particular interest since some physics observables, e.g. the like-sign particle interferometry rely on accurate recording of particles with small momentum differences. Fig. 11 shows the detection probability as a function of distance between the chamber coordinates in horizontal and vertical direction of an observed track and all other nearby tracks. The plateaus have been normalized to the average detection efficiency. The vicinity of tracks is defined in the x-direction within a narrow y-window (± 17 mm) and in the y-direction within a narrow x-window (± 2 mm). The resulting distribution of differences in the x-direction should be flat (except for physics effects of e.g. particle interference) if all tracks were recorded. Only tracks observed in all four tracking planes are included in this analysis. The resulting two-track resolution can be derived from Fig. 11. At 5 mm distance in the x-direction a track may be observed with 50% chance while the probability increases to the average detection efficiency at a distance of 7 mm. In the vertical direction the two-track resolution is worse due to the much longer pad dimension (17 mm). The momentum difference between two particles corresponding to the minimum distance 7 mm is about 2 and 13 MeV/c, for pion pairs at 1 and 8 GeV/c, respectively.

7. Acceptance

In a magnetic spectrometer the acceptance in momentum is the same for different particle masses of the same charge. The transverse momentum (p_T)

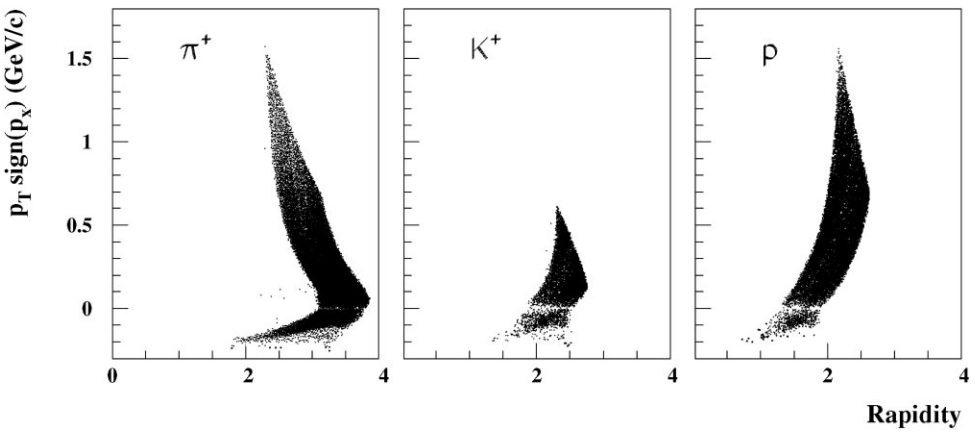

Fig. 12. Acceptance in terms of p_T and rapidity for pions, kaons and protons in data.

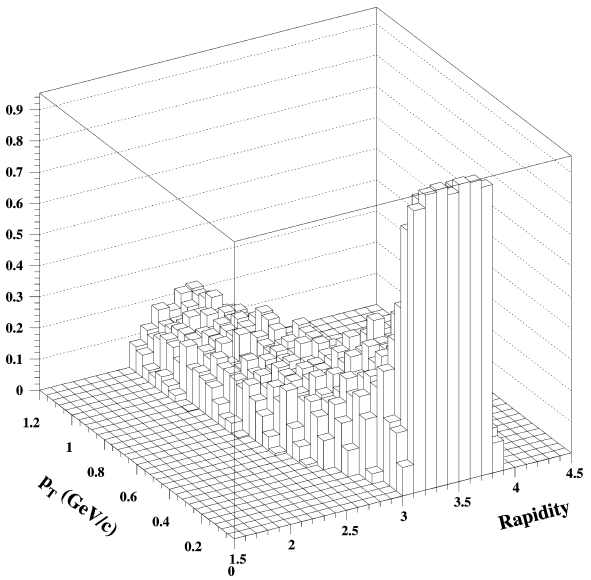

Fig. 13. Simulated detection probability in p_T versus rapidity due to geometrical acceptance for pions with positive p_x.

and rapidity (y) are relevant kinematic observables in high-energy physics experiments. Expressed in these variables the regions of acceptance differ for different particle masses. This is a nuisance since one prefers to compare data at the same rapidity, i.e. in the same kinematic regime which defines the source of the observed particles.

The particle-dependent acceptance regions are evident in Fig. 12 which shows the location in the p_T–y plane for the different particle species. The sign(p_x) factor is introduced for clarification, as it unfolds the spectrum for particles with negative p_x and momentum low enough to bend over the beam line.

Inside each acceptance region the acceptance correction is strongly dependent on y and p_T as illustrated in Fig. 13 which shows the detection probability for pions as it is simulated by GEANT. The acceptance correction can be qualitatively understood by considering particles with p_T near 0. For these particles, if the momentum is such that they enter the arm, the azimuthal coverage will be 2π. Particles with larger p_T, only weakly influenced by the magnetic field, will have an acceptance approaching the geometric azimuthal coverage of the tracking arm.

8. Concluding remarks

The described tracking system covers a large detection area with four planes of space-point measuring tracking detectors and a high-resolution time of flight wall. The system has been exploited for data taking in the 158 A GeV Pb-beam with typically 30 charged particles passing through the tracking system in a central Pb + Pb collision.

For the most central collisions, the track density at the small-angle side of the system approaches $100/m^2$ which is comparable to the expected situation in heavy-ion experiments at RHIC and LHC. The possibility to perform straight-line tracking at this particle density using only four space points along the track was demonstrated. Reliable tracking is achieved, in spite of the minimal redundancy, since each point is unambiguously determined and the coordinates are determined with high resolution in both dimensions which allows a restrictive track definition. The momentum resolution was in the range 1–3%. π/K separation was achieved up to 4 GeV/c and p/π separation up to 8 GeV/c.

The system has proven to produce reliable tracking results at high particle densities. The performance of found tracks and particle identification could be demonstrated already online. The offline analysis which is now in an advanced stage, has proven that high-quality spectra of π, K, p and their respective antiparticles, can be obtained. Moreover, results on Δ^{++} and ϕ-meson production (together with arm 1) are obtainable as well as particle correlation studies between pairs of protons, kaons and pions.

Acknowledgements

This work was supported by the Swedish National Science Research Council (NFR), the Swedish Board for Planning and Coordination of Research (FRN), the Dutch Stichting voor Fundamenteel Onderzoek der Materie (FOM), the Swiss National Fund, the Japanese Grant-in-Aid for Scientific Research (Specially promoted Research & International Scientific Research) of the Ministry of Education, Science and Culture and the University of Tsukuba Special Research Projects, JSPS Research Fellowships for Young Scientists.

References

[1] M.M. Aggarwal et al., (WA98 collaboration), in preparation.
[2] L. Carlén et al., Nucl. Instr. and Meth. A 391 (1997) 492.
[3] L. Carlén et al., Nucl. Instr. and Meth. A 413 (1998) 92.
[4] L. Carlén et al., Nucl. Instr. and Meth. A 412 (1998) 361.
[5] R. Albrecht et al., Z. Phys. C 55 (1992) 539.
[6] R. Albrecht et al., Nucl. Inst. and Meth. A 276 (1989) 131.
[7] T. Chujo et al., Nucl. Instr. and Meth. A 393 (1996) 409.
[8] PHENIX Conceptual Design Report, BNL 1993 (unpublished).
[9] H. Sorge, Phys. Rev. C 52 (1995) 3291.
[10] R. Brun, F. Carminati, GEANT Detector Description and Simulation Tool, CERN Program Library, Long Writeup W5013, March 1994.